

2

## REPORT DOCUMENTATION PAGE

AD-A235 297



1d. RESTRICTIVE MARKINGS N/A									
3. DISTRIBUTION/AVAILABILITY OF REPORT Approved for public release, distribution unlimited.									
4. PERFORMING ORGANIZATION REPORT NUMBER(S) Technical Report No. 7									
5. MONITORING ORGANIZATION REPORT NUMBER(S)									
6a. NAME OF PERFORMING ORGANIZATION University of California Berkeley	6b. OFFICE SYMBOL (If applicable)								
7a. NAME OF MONITORING ORGANIZATION Office of Naval Research									
6c. ADDRESS (City, State and ZIP Code) Chemistry Department University of California Berkeley, CA 94720	7b. ADDRESS (City, State and ZIP Code) 800 N. Quincy St. Arlington, VA 22217								
8a. NAME OF FUNDING/SPONSORING ORGANIZATION Office of Naval Research	8b. OFFICE SYMBOL (If applicable)								
8. PROCUREMENT INSTRUMENT IDENTIFICATION NUMBER N0014-87-K-0495									
9a. ADDRESS (City, State and ZIP Code) 800 N. Quincy St. Arlington, VA 22217	10. SOURCE OF FUNDING NOS.								
	<table border="1"> <thead> <tr> <th>PROGRAM ELEMENT NO.</th> <th>PROJECT NO.</th> <th>TASK NO.</th> <th>WORK UNIT NO.</th> </tr> </thead> <tbody> <tr> <td></td> <td></td> <td></td> <td></td> </tr> </tbody> </table>	PROGRAM ELEMENT NO.	PROJECT NO.	TASK NO.	WORK UNIT NO.				
PROGRAM ELEMENT NO.	PROJECT NO.	TASK NO.	WORK UNIT NO.						
11. TITLE (Include Security Classification): Negative Ion Photo-detachment as a Probe of the Transition State Region: The I + HI Reaction									
12. PERSONAL AUTHOR(S) D. M. Neumark									
13a. TYPE OF REPORT Interim Technical	13b. TIME COVERED FROM 4/1/91 TO 4/30/91								
14. DATE OF REPORT (Yr., Mo., Day) 91/4/30	15. PAGE COUNT 40								
16. SUPPLEMENTARY NOTATION To be published in <u>Advances in Molecular Vibrations and Collision Dynamics</u> , Vol. 1 (JAI Press, Inc., Greenwich, CT, 1991), pp. 165-185.									
17. COSATI CODES	18. SUBJECT TERMS (Continue on reverse if necessary and identify by block number)								
<table border="1"> <thead> <tr> <th>FIELD</th> <th>GROUP</th> <th>SUB GR</th> </tr> </thead> <tbody> <tr> <td></td> <td></td> <td></td> </tr> </tbody> </table>	FIELD	GROUP	SUB GR				photodetachment, transition states, clusters		
FIELD	GROUP	SUB GR							
19. ABSTRACT (Continue on reverse if necessary and identify by block number)									
<p>The study of the transition state of bimolecular reactions using negative ion photo-detachment is described. The I + HI reaction is used as an example of this method. The photoelectron spectrum of IHI<sup>-</sup> shows resolved vibrational features assigned to a progression in the antisymmetric stretch mode of the neutral IHI complex. Threshold photodetachment studies of this system at higher resolution show additional structure that arises from two sources: (1) resonances supported by the I + HI potential energy surface and (2) transitions to nearly free internal rotor states of the IHI complex. The photoelectron spectrum of the cluster anion IDI<sup>-</sup>(N<sub>2</sub>O) is also described.</p>									
20. DISTRIBUTION/AVAILABILITY OF ABSTRACT UNCLASSIFIED/UNLIMITED <input checked="" type="checkbox"/> SAME AS RPT. <input type="checkbox"/> DTIC USERS <input type="checkbox"/>	21. ABSTRACT SECURITY CLASSIFICATION Unclassified								
22a. NAME OF RESPONSIBLE INDIVIDUAL Dr. David L. Nelson	22b. TELEPHONE NUMBER (Include Area Code) (202) 696-4410								
	22c. OFFICE SYMBOL								

OFFICE OF NAVAL RESEARCH

Contract # N0014-87-K-0495

R&T Code 400X026  
Technical Report No. 7

Negative Ion Photodetachment as a Probe of the  
Transition State Region: The I + HI Reaction

by

Daniel M. Neumark



To be published in  
*Advances in Molecular Vibrations and Collision Dynamics*, Vol. 1  
(JAI Press, Inc., Greenwich, CT, 1991), pp. 165-185

Department of Chemistry  
University of California  
Berkeley, CA 94720

April 30, 1991

CLASSIFICATION	
UNCLASSIFIED	<input checked="" type="checkbox"/>
CONFIDENTIAL	<input type="checkbox"/>
SECRET	<input type="checkbox"/>
RESTRICTED	
By	
Date	
Availability Code	
Dist. Statement	
Dist. Restrictions	
Notes	
A-1	

Reproduction in whole, or in part, is permitted for  
any purpose of the United States Government.

This document has been approved for public release and sale:  
its distribution is unlimited.

91 4 25 060

Negative Ion Photodetachment as a Probe of the Transition State

Region: The I + HI Reaction

Daniel M. Neumark\*  
Department of Chemistry  
University of California  
Berkeley, CA 94720

1. Introduction
2. Experimental
3. Results and Discussion
  - a)  $\text{IHI}^-$  Photoelectron Spectrum
  - b) Threshold Photodetachment Spectroscopy of  $\text{IHI}^-$
  - c)  $\text{IDI}^-(\text{N}_2\text{O})$  Photoelectron Spectrum
4. Summary
5. Acknowledgments

---

\* NSF Presidential Young Investigator and Alfred P. Sloan Fellow

## INTRODUCTION

Experimental investigations of molecular vibrations can be split into studies of bound and unbound systems. In the case of bound systems, the emphasis in recent years has been on improving spectral resolution in order to better understand the vibrational motion of molecules and clusters. For unbound systems, dynamical as well as spectroscopic issues are of importance. A vital dynamical question is whether the lifetime of the system of interest with respect to, for example, dissociation or electron ejection is sufficiently long so that any resolved vibrational structure can be observed. If this condition is satisfied, then one can use the observed peak positions and linewidths to learn about both the spectroscopy and dynamics of the unbound system. The literature abounds with examples of this in studies of predissociating,<sup>1</sup> autoionizing,<sup>2</sup> and autodetaching<sup>3</sup> systems.

In this chapter, we discuss experiments in our laboratory which probe the vibrational motion associated with an unbound system of paramount importance in chemical physics: the transition state of a chemical reaction. These 'transition state spectroscopy' experiments allow the powerful techniques of spectroscopic analysis to be applied to the study of the potential energy surfaces that govern chemical reactions. Our experiments are based on the idea that the transition state region of the potential energy surface for a neutral bimolecular reaction can be accessed by photodetaching a stable negative ion, so long as the geometry of the negative ion is similar to that of

the neutral transition state. We define the 'transition state region' of a potential energy surface to be the region of the surface where the properties of the complex formed in a reactive collision are distinct from separated reactants or products; this definition broadly covers the region where chemical bond cleavage and formation occurs, and is intended to be more general than the classical definition of the transition state in transition state theory.

a) Background

Before describing our photodetachment experiments in detail, it is instructive to discuss some of the previous and ongoing investigations in the field of transition state spectroscopy. The goal of these studies is to probe the transition state region directly, rather than simply measure product distributions as is typically done in state-to-state scattering experiments. Transition state spectroscopy can be divided into 'full collision' experiments, in which one attempts to study the short-lived complex formed in a reactive collision, and 'half-collision' experiments in which a repulsive or reactive potential energy surface is probed via photoexcitation of a bound species. In principle, 'full collision' experiments are more general because reactive collisions, by definition, must sample the transition state region of the potential energy surface. In 'half collision' experiments, one must be certain that the initial bound species has good geometric overlap with the

transition state region of the surface accessed via photoexcitation. However, 'half collision' experiments often allow one to probe the transition state region under better-defined initial conditions than 'full collision' experiments.

The first transition state spectroscopy experiments were the full collision studies of Polanyi,<sup>4</sup> Brooks,<sup>5</sup> and their co-workers in 1980. Polanyi reported the observation of chemiluminescence from the F-Na-Na complex formed in the  $F + Na_2$  reaction. In Brooks's experiments, which have focussed on the reaction  $K + NaCl \rightarrow Na + KCl$ ,<sup>6</sup> the  $[KNaCl]$  complex formed in the is electronically excited with a tunable laser, and the  $Na^*$  which results from decomposition of the  $[KNaCl]^*$  complex is monitored by emission. Experiments of this type have also been performed by Kompa<sup>7</sup> and Burnham,<sup>8</sup> in which laser excitation of the  $[XeCl_2]$  complex formed in a  $Xe + Cl_2$  collision yields emission from  $XeCl^*$ , and by Kleiber et al.<sup>9</sup> on the  $Mg + H_2$  reaction. Morgner has used Penning ionization to probe the complex formed in collisions of metastable He with halogen molecules.<sup>10</sup> The most intriguing 'full collision' transition state spectroscopy experiments have been performed by Valentini and co-workers.<sup>11</sup> Their state-resolved measurements on the  $H + H_2$  and  $D + H_2$  reactions show evidence for reactive resonances associated with quasi-bound states of the  $[H_3]$  complex. These experiments, which are described in detail elsewhere in this volume, are the only 'full collision' studies which show any hint of vibrational structure associated with the transition state.

With the exception of Valentini's experiment, the full collision experiments described above require laser excitation of an extremely short-lived collision complex ( $<10^{-13}$  sec) under the poorly-defined initial conditions typical of a scattering experiment: neither reactant orientation nor total angular momentum is well-defined. Thus, in addition to the experimental difficulties involved in observing such a short-lived species, the electronic spectroscopy of these species is expected to be complex and difficult to interpret.

These problems are mitigated to some extent in 'half collision' studies. In one class of these experiments, photoexcitation of a stable van der Waals molecule is used to initiate a reaction on either a ground or excited state potential energy surface. Wittig and co-workers<sup>12</sup> studied the reaction  $H + CO_2 \rightarrow OH + CO$  via photodissociation at 193 nm of the HBr entity in the van der Waals molecule  $CO_2 \cdot HBr$ ; this restricts the range of reactant orientations contributing to reaction and the resulting OH product state distribution differs from the conventional bimolecular reaction of the same translational energy. Breckenridge et al.<sup>13</sup> have used excitation of the  $Hg \cdot H_2$  van der Waals molecule to access the potential energy surface for the excited state reaction  $Hg(^3P_1) + H_2 \rightarrow HgH + H$ . By monitoring the HgH product yield as a function of the laser frequency used to excite the  $Hg \cdot H_2$  complex, they obtain structured 'action spectra' characteristic of the  $[HgH_2]^*$  complex on the reactive potential energy surface. In another important set of 'half

collision' experiments, performed by Imre et al.,<sup>14</sup> Kleinermanns,<sup>15</sup> and Butler,<sup>16</sup> a stable molecule is excited to a repulsive electronic potential energy surface and the dispersed fluorescence from the dissociating fragments is observed. The vibrational progressions in the dispersed fluorescence spectra are sensitive to the dynamics on the excited state surface.

The above experiments are examples of frequency-resolved 'half-collision' studies. Zewail and co-workers<sup>17, 18</sup> have pioneered the development of time-resolved 'half-collision' experiments in which femtosecond laser pulses are used to monitor the progress of a chemical reaction in real time. For example, they have performed pump and probe experiments on the  $\text{CO}_2\cdot\text{HI}$  complex<sup>17</sup> in which the first laser pulse initiates reaction within the complex via photodissociation of the  $\text{HBr}$ , and the second pulse monitors the appearance of the  $\text{OH}$  product as a function of time. This provides a 'real-time clock' of the  $\text{H} + \text{CO}_2$  reaction. Real time pump and probe experiments have also been used to study the photodissociation of  $\text{ICN}$  and  $\text{HgI}_2$ .<sup>18</sup> In these experiments, the photofragments are monitored in the transition state region as well as the asymptotic region of the potential energy surfaces on which dissociation occurs. By determining how the spectroscopy of the nascent photofragments evolves as the reaction proceeds, one can, in principle, obtain a very detailed description of the dissociation process.

b) Photodetachment probes of the transition state

We have developed a 'half-collision' experiment which draws on several of the ideas developed in the experiments described above. Our experiment also draws on earlier work by Lineberger<sup>19</sup> and Brauman,<sup>20</sup> in which photodetachment of a stable anion results in a neutral species unstable with respect to either isomerization or dissociation. In our experiments, a stable negative ion serves as the precursor to the transition state of a neutral bimolecular reaction. This method is most suitable for the study of hydrogen transfer reactions  $A + HB \rightarrow HA + B$ , where A and B can be atomic or polyatomic species. We can then probe the unstable [AHB] complex formed in the reaction by photodetaching the stable, hydrogen-bonded negative ion  $AHB^-$ .<sup>21</sup> If the ion geometry is similar to that of the neutral transition state, then photodetaching the ion will probe the transition state region of the A + HB potential energy surface. Even though the [AHB] complex is unstable, the photoelectron spectrum of  $AHB^-$  can exhibit resolved vibrational structure which yields considerable insight into the spectroscopy and dissociation dynamics of the [AHB] complex. Hydrogen transfer reactions are particularly appealing because, in many cases, the transition state region for the reaction has good geometric overlap with the strongly hydrogen-bonded ion  $AHB^-$ . In addition, most hydrogen transfer reactions are 'Heavy + Light-Heavy' reactions, in which a hydrogen atom is transferred between two much heavier species. The dissociation dynamics of the [AHB] complex with this mass

combination favors the observation of resolved vibrational structure in the  $AHB^-$  photoelectron spectrum. In essence, we observe the fast vibrational motion of the light H atom as the complex slowly dissociates.

This experiment provides a high degree of control over important parameters of a chemical reaction. Photodetachment initiates the  $A + HB$  reaction with the atoms in the same geometry as they are in the ion  $AHB^-$ , thereby providing excellent control over the reactant orientation. In addition, since the ions are generated in a source which produces rotationally cold species, we can limit the total angular momentum available to the reaction. The latter restriction is particularly significant since it facilitates comparison with theoretical simulations of our results.

The simplest reactions amenable to this method are those in which a hydrogen atom is exchanged between two like or unlike halogen atoms. We have presented results on the symmetric reactions  $Cl + HCl$ ,<sup>22</sup>  $I + HI$ ,<sup>23</sup> and  $Br + HBr$ <sup>24</sup> which were studied via photoelectron spectroscopy of  $ClHCl^-$ ,  $BrHBr^-$ , and  $IHI^-$ . The photoelectron spectra of these ions show resolved vibrational progressions assigned on the basis of isotope shifts to the  $\nu_3$  antisymmetric stretch vibration of the unstable  $[XHX]$  complex. This vibration involves H atom motion between two essentially stationary halogen atoms and is poorly coupled to the dissociation coordinate of the complex. The spectra show large 'red shifts' in the  $\nu_3$  mode relative to diatomic  $HX$ , indicating

that photodetachment indeed accesses the transition state region on the X + HX potential energy surface where the H atom is interacting strongly with both X atoms. Simulations of these photoelectron spectra on model X + HX potential energy surfaces<sup>23,24,25,26,27</sup> show that they are quite sensitive to the nature of the transition state region.

In a similar vein, the photoelectron spectra of asymmetric XHY<sup>-</sup> bihalide anions allows us to probe asymmetric exchange reactions including  $\text{Br} + \text{HI} \rightarrow \text{HBr} + \text{I}$ ,  $\text{Cl} + \text{HI} \rightarrow \text{HCl} + \text{I}$ , and  $\text{F} + \text{HI} \rightarrow \text{HF} + \text{I}$ .<sup>28,29</sup> These spectra also show progressions in the  $\nu_3$  mode of the [XHY] complex, although they provide more information on the I + HX product valley of the neutral potential energy surface than on the region near the entrance channel barrier. Finally, we have studied hydrogen transfer reactions such as  $\text{F} + \text{CH}_3\text{OH} \rightarrow \text{HF} + \text{CH}_3\text{O}$  which involve polyatomic reactants.<sup>30</sup> The photoelectron spectrum of  $\text{CH}_3\text{OHF}^-$  again shows vibrational structure assigned to H atom motion between the O and F atoms in the [CH<sub>3</sub>OHF] complex.

One feature common to all the photoelectron spectra mentioned above is that the widths of the observed transitions is broader than the experimental resolution. An important question concerning the dissociation dynamics of the neutral complex is the following. Are the peak widths determined solely by the 'lifetime' of the neutral complex, or is there underlying structure which is unresolved in the photoelectron spectra? This question is particularly intriguing with reference to the  $\text{BrHBr}^-$

and  $\text{IHI}^-$  spectra which show widely varying peak widths. In order to answer this, we have recently constructed a threshold photodetachment spectrometer<sup>31</sup> with considerably higher resolution than the instrument on which the photoelectron spectra were obtained. The principles behind the two types of measurements are discussed in the following section.

This article focuses on the reaction that has been most amenable to study via negative ion photodetachment: the  $\text{I} + \text{HI}$  reaction. We review our previously published photoelectron spectroscopy work<sup>23</sup> on  $\text{IHI}^-$  and compare it to new higher resolution results.<sup>32</sup> The newer results indeed reveal fine structure in the  $[\text{IHI}]$  complex that was obscured at lower resolution. This structure provides definitive evidence for the existence of dynamical resonances in the  $\text{I} + \text{HI}$  reaction. We conclude by presenting results on the photoelectron spectroscopy of the cluster ion  $\text{IDI}^-(\text{N}_2\text{O})$ ,<sup>29</sup> which represents the first step in determining how a bihalide ion photoelectron spectrum evolves upon the addition of solvating species.

## EXPERIMENTAL

The spectra shown below were obtained with two negative ion photodetachment methods: 'fixed-frequency' photoelectron spectroscopy<sup>33</sup> and threshold photodetachment spectroscopy. The instruments used in these studies have been described in detail previously.<sup>24,31,34</sup> In this section we wish only to describe the

principles behind each experiment.

In both experiments, negative ions are generated by expanding a mixture of neutral gases (10% HI in Ar for the results shown here) through a pulsed molecular beam valve, and by crossing the molecular beam with a 1 keV electron beam just outside the valve orifice.<sup>35</sup> This results in the formation of ions in the continuum flow region of the supersonic expansion and the ions should cool internally as the expansion progresses. Negative ions are extracted from the beam, accelerated to 1 keV and mass-selected using time-of-flight mass spectroscopy.<sup>36,37</sup> In our photoelectron spectrometer, the mass-selected ions are photodetached with a pulsed, fixed-frequency laser. The results shown below were obtained with the fourth harmonic of a Nd:YAG laser at a photon energy of 4.66 eV ( $\lambda = 266$  nm). We then determine the electron kinetic energy distribution of a small fraction of the ejected photoelectrons by time-of-flight. For a single photodetachment event, the electron kinetic energy (eKE) is given by

$$eKE = h\nu - E_b^- - E_{int}^0 + E_{int}^- . \quad (1)$$

Here  $h\nu$  is the photon energy and  $E_b^-$  is the binding energy of the electron to the anion. This is 3.80 eV for  $IHI^-$ , which is the energy required to remove an electron from the ground state of  $IHI^-$  to form  $I + HI(v=0)$ .  $E_{int}^-$  and  $E_{int}^0$  are the internal energies of the anion and neutral, respectively. Thus, the electron kinetic energy distribution exhibits peaks resulting from transitions between ion and neutral energy levels. In nearly all

cases, the energy resolution of photoelectron spectroscopy is insufficient to discern rotational structure and one only learns about vibrational energy levels of the neutral and (occasionally) the anion. In our spectrometer, for example, the resolution is 8 meV at  $eKE = 0.65$  eV and degrades at higher electron kinetic energies as  $(eKE)^{3/2}$ .

Considerably higher energy resolution can be achieved with threshold photodetachment spectroscopy. In this experiment, the ions are photodetached with a tunable pulsed dye laser. At a given laser wavelength, only electrons produced with nearly zero-kinetic energy are detected. The zero-kinetic energy spectrum plotted as a function of laser wavelength consists of a series of peaks, each corresponding to an ion-neutral transition. The width of the peaks is determined by the ability of the instrument to discriminate against photoelectrons produced with high kinetic energy. By adapting the methods developed by Müller-Dethlefs et al. for threshold photoionization of neutrals,<sup>38</sup> we have achieved a resolution of  $3 \text{ cm}^{-1}$  (0.37 meV) with this instrument and were able to obtain a spectrum of  $\text{SH}^-$  in which transitions between individual rotational levels of the anion and neutral were resolved.<sup>31</sup> In the experiments performed on  $\text{IHI}^-$ , tunable laser light in the range of 300 nm was required. This was obtained by frequency doubling the output of an excimer pumped dye laser running at 50 Hz. Three laser dyes, rhodamine 590, 610, and 640, were required to cover the frequency range of interest. Frequency doubling was done with a KDP or BBO crystal,

resulting in pulse energies of 3-5 mJ. The operating conditions used in the  $\text{IHI}^-$  studies resulted in an energy resolution of 1-2 meV.

## RESULTS AND DISCUSSION

### a) $\text{IHI}^-$ Photoelectron Spectrum

The photoelectron spectrum of  $\text{IHI}^-$  is shown in Figure 1. The spectrum shows three peaks, all of which lie at electron kinetic energies below  $h\nu - E_b^- = 0.86$  eV, the kinetic energy that would result if  $\text{I} + \text{HI}(v=0)$  were formed. This value is derived from the laser photon energy (4.66 eV), the electron affinity of iodine (3.0591 eV<sup>39</sup>), and the enthalpy of dissociation of  $\text{IHI}^-$  into  $\text{I}^- + \text{HI}(v=0)$  ( $0.74 \pm 0.13$  eV<sup>40</sup>). Thus, all the peaks correspond to states of the  $[\text{IHI}]$  complex with sufficient energy to dissociate to  $\text{I} + \text{HI}(v=0)$ . In the photoelectron spectrum of  $\text{IDI}^-$  (Figure 2), three peaks are also observed. The peak at highest electron kinetic energy does not shift, but the spacing between the peaks is less. On this basis, the peaks are assigned to a progression in the  $v_3$  antisymmetric stretch vibration of the neutral  $[\text{IHI}]$  complex originating from the  $v_3'' = 0$  level of  $\text{IHI}^-$ . Since this is not a totally symmetric vibration, only transitions to even  $v_3'$  levels of  $[\text{IHI}]$  are allowed. The peaks are therefore due to transitions to the  $v_3' = 0, 2,$  and  $4$  antisymmetric stretch levels of  $[\text{IHI}]$ . The spectrum shows that the  $v_3' = 0$  and  $v_3' = 2$  levels of the complex are separated by 0.174 eV, which is considerably smaller than the HI

vibrational frequency ( $0.286 \text{ eV}^4$ ). Hence we are probing a region of the potential energy surface where the H atom is vibrating in a much flatter potential than in diatomic HI; this is a signature of the transition state region where the H atom interacts strongly with both I atoms.

An interesting feature in the  $\text{IHI}^-$  and  $\text{IDI}^-$  photoelectron spectra is the wide variation in the observed peak widths. The widths (FWHM) of the  $v_3' = 0, 2, \text{ and } 4$  peaks in the  $\text{IHI}^-$  spectrum are 74 meV, 23 meV, and ~50 meV, respectively, while the widths of the corresponding peaks in the  $\text{IDI}^-$  spectrum are 50 meV, 42 meV, and 13 meV. While one might be tempted to attribute the peak widths to lifetime broadening of the various  $v_3'$  levels of the neutral complex, this is a dangerous assumption. The peak widths do not appear to depend in an intuitively simple way on the internal energy of the complex. For example, of the three peaks in the  $\text{IDI}^-$  spectrum, the narrowest (the  $v_3' = 4$  peak) results from the state of the  $[\text{IDI}]$  complex with the most internal energy. The pattern of the peak widths suggests the possibility that at least some of the peaks are envelopes of transitions which are not resolved in the photoelectron spectrum.

To gain further insight into the  $\text{IHI}^-$  and  $\text{IDI}^-$  photoelectron spectra, the spectra have been simulated at various levels of approximation by three different groups.<sup>23,25,26,27</sup> The simulations consist of calculating the Franck-Condon overlap as a function of energy between the ion and the scattering wavefunctions supported by a model I + HI potential energy surface. All three

simulations use the same I + HI surface,<sup>42</sup> a LEPS (London-Eyring-Polanyi-Sato<sup>43</sup>) surface with a collinear minimum energy path and a 1.1 kcal/mol barrier at the saddle point. The same IHI<sup>-</sup> geometry and vibrational frequencies are also used. The ion is assumed to be linear and centrosymmetric<sup>44</sup> with an equilibrium interiodine distance of 3.88 Å, and the vibrational frequencies are taken from matrix isolation spectroscopy.<sup>21</sup> In the simulations performed by our group,<sup>23</sup> the bending motion of the ion and complex was neglected and only the symmetric ( $\nu_1$ ) and antisymmetric ( $\nu_3$ ) stretch vibrations are considered. This was considered a reasonable approximation because the combination of a linear ion and a neutral surface which favors the collinear [IHI] geometry leads one to expect little or no bending excitation in the photoelectron spectrum. Gazdy and Bowman<sup>27</sup> have performed three-dimensional simulations of the spectra which include the bending motion and use an  $L^2$  basis for the scattering wavefunctions. Schatz<sup>25</sup> has simulated the spectra using the exact three-dimensional wavefunctions supported by the I + HI surface. All the simulations assume the ion is in its ground vibrational state and that the total angular momentum  $J = 0$  for the ion and neutral complex.

In all the simulations, the  $\nu_3' = 2$  and 4 features in the IHI<sup>-</sup> and IDI<sup>-</sup> spectra appear not as single broad peaks, but rather as progressions of peaks spaced by about 12 meV (100 cm<sup>-1</sup>). The closely spaced peaks represent transitions to metastable symmetric stretch levels of the complex. For example,

the simulation by Schatz, which is the most realistic, shows three closely spaced peaks associated with the  $v_3 = 2$  level of [IHI] resulting from transitions to the  $v_1 = 0, 1, \text{ and } 2$  symmetric stretch levels of the complex. The linewidths of these peaks are 2-5 meV, indicating lifetimes of several hundred femtoseconds for these metastable states. These relatively long-lived states are responsible for the sharp resonance structure predicted in quantum mechanical reactive scattering calculations on Heavy + Light-Heavy reactions,<sup>45,46,47</sup> of which I + HI is an extreme example. On the other hand, the transition to the  $v_3 = 0$  level of [IHI] (and [IDI]) is predicted to be dominated by overlap with direct scattering wavefunctions; the  $v_3' = 0$  level of the complex formed by photodetachment dissociates rapidly. Nonetheless, even the simulated  $v_3' = 0$  feature in Schatz's simulation consists of a series of peaks rather than a single broad peak. In summary, a comparison of the experimental and simulated photoelectron spectra strongly suggests that the peaks in the experimental spectra are envelopes for unresolved underlying structure which, if observable, would provide yet another level of insight into the transition state region of the I + HI reaction. The possibility of observing this underlying structure motivated the higher resolution experiments discussed in the next section.

#### b) Threshold Photodetachment Spectroscopy of $\text{IHI}^-$

The threshold photodetachment spectra of the three peaks in

Figure 1 are shown in Figures 3-5. The horizontal axis at the bottom of each plot shows the photodetachment wavelength  $\lambda$ . For convenient comparison with Figure 1, the top axis shows the corresponding electron kinetic energy (eKE) that would result in a photoelectron spectrum at 266 nm; the two axes are related by  $eKE = 1240(1/266 - 1/\lambda)$ .

The threshold photodetachment spectrum of the  $v_3' = 2$  peak (Figure 3) reveals three partially resolved peaks spaced by approximately 12 meV. The peak widths are about 12 meV, and the intensity of the peaks decreases towards lower wavelength. The observed peak spacing is in the range expected for a progression in symmetric stretch levels of the [IHI] complex. In fact, the experimental peak spacings and intensities are quite similar to the simulations of the  $v_3' = 2$  feature. The major difference is that in the simulation by Schatz,<sup>25</sup> the peaks in the symmetric stretch progression are narrower (2 meV) and are therefore fully resolved. Nonetheless, the correspondence between the experimental and simulated spectra strongly suggests we are seeing a progression in quasi-bound [IHI] symmetric stretch states.

Figure 4 shows the threshold photodetachment spectrum of the  $v_3'=4$  feature in the  $\text{IHI}^-$  photoelectron spectrum. Four well-resolved peaks are evident in this spectrum. Peaks A, a, and b are evenly spaced by an interval of 16.0 meV (129  $\text{cm}^{-1}$ ), while peaks A and B are separated by 12.5 meV (101  $\text{cm}^{-1}$ ). The peaks are substantially narrower than those in Figure 3; peaks A

and a are 3.7 meV wide, and peak B is 5.6 meV wide.

The presence of two intervals among the peaks in Figure 4 suggests the presence of two progressions. We find that the intensities of peaks a and b are sensitive to the ion source operating conditions. For example, their intensities relative to peaks A and B increase if a 10% HI/He mixture is expanded through the pulsed molecular beam valve instead of the 10% HI/Ar mixture used in the results shown here. In addition, matrix isolation studies<sup>21</sup> on  $\text{IHI}^-$  have yielded a value of  $129 \text{ cm}^{-1}$  for the symmetric stretch frequency in the ion, in excellent agreement with the spacing between peaks A, a, and b. We therefore assign peaks a and b to hot band transitions originating from the  $v_1'' = 1$  and  $v_1'' = 2$  symmetric stretch levels of the ion and terminating in the same level of the neutral as peak A. The a/A intensity ratio yields a vibrational temperature of 100 K for the  $\text{IHI}^-$  ions.

Peaks A and B belong to a second progression. The peak spacing and widths agree with what the simulations predict for transitions to metastable  $[\text{IHI}]$  levels. The peaks are assigned to transitions between the  $v_1'' = 0$  level of the ion and two different symmetric stretch levels of the  $[\text{IHI}]$  complex. This assignment is consistent with the noticeably different peak widths which imply that the transitions are to two distinct levels of the complex with different lifetimes. The widths yield lower bounds of 180 and 120 fs for the upper state lifetimes of A and B, respectively. Since the symmetric stretch vibration of

[IHI] is strongly coupled to the dissociation coordinate of the complex, it seems reasonable that the higher lying symmetric stretch level of the complex (peak B) should have a shorter lifetime. Similar trends have been observed in collinear scattering calculations on the  $\text{Cl} + \text{HCl}^{48}$  and  $\text{F} + \text{DBr}^{49}$  reactions. Note that a substantial portion of the width of peak A is due to the experimental resolution, so the upper state lifetime for this transition may be considerably longer.

The symmetric stretch levels of the [IHI] complex with  $v_3' = 4$  lie 0.49 eV above the  $\text{I} + \text{HI}$  ( $v = 0$ ) asymptote compared to 0.30 eV for the levels with  $v_3' = 2$ . The peak widths in Figures 3 and 4, however, indicate that the lifetimes of the  $v_3' = 4$  levels are considerably longer, a striking and somewhat non-intuitive result. However, the  $v_3$  antisymmetric stretch mode is poorly coupled to the dissociation coordinate of the [IHI] complex, so it is not necessary that increased excitation in this mode should result in shorter lifetimes for the metastable states. In recent three-dimensional simulations of the  $\text{IDI}^-$  photoelectron spectrum, Schatz<sup>50</sup> found that transitions to [IDI] symmetric stretch levels with  $v_3' = 4$  were indeed narrower than those to  $v_3' = 2$ . This effect clearly calls for further experimental and theoretical study.

We conclude this section by considering the threshold photodetachment spectrum for the transition to  $v_3' = 0$  which is shown in Figure 5. The single broad peak in the photoelectron spectrum actually consists of a series of peaks spaced by an

interval that increases from 20 meV to 25 meV towards lower laser wavelength. This is quite distinct from the 12 meV interval seen in the other spectra. However, as discussed above, the simulations predict a qualitatively different interpretation for the  $v_3' = 0$  feature in the  $\text{IHI}^-$  photoelectron spectrum. In contrast to the  $v_3' = 2$  and 4 levels of  $[\text{IHI}]$ , photodetachment to  $v_3' = 0$  is expected to primarily access direct scattering  $\text{I} + \text{HI}$  wavefunctions rather than quasi-bound resonances. We must therefore search for another explanation for structure in the  $v_3' = 0$  transition. Figure 5 shows that there is an approximate correspondence between the peak positions and the energetic thresholds for the asymptotic levels  $\text{I} + \text{HI}(v=0, j = 11-16)$ . The thresholds for these asymptotic states are indicated in Figure 5. The thresholds in figure 5 are drawn assuming the threshold for  $\text{I} + \text{HI}(v=0, j=0)$  is at 3.79 eV, well within the error bars of the value of  $E_b^-$  for  $\text{IHI}^-$ ,  $3.80 \pm 0.13$  eV, used above. Our results therefore indicate that photodetachment to  $\text{I} + \text{HI}(v=0, j)$  is enhanced near the thresholds for formation of HI in high rotational states.

In his three-dimensional simulation of the  $\text{IHI}^-$  photoelectron spectrum, Schatz<sup>25</sup> also observed peaks in the transitions to  $v_3' = 0$  levels of the complex which correspond to asymptotic  $\text{I} + \text{HI}$  rotational energy levels. However, his results show significant intensity down to the  $\text{I} + \text{HI}(j=0)$  level. The apparent drop in signal for  $j < 11$  may indicate that on the real  $\text{I} + \text{HI}$  potential energy surface, the scattering wavefunctions

which asymptotically correlate to I + HI ( $v=0$ ,  $j<11$ ) do not have much amplitude in the region of the surface probed by photodetachment. This may indicate that low rotational states of HI( $v=0$ ) are relatively unreactive; if relatively few I + HI ( $v=0$ ,  $j<11$ ) collisions lead to reaction, then the corresponding scattering wavefunctions will not penetrate into the transition state region. Classical trajectory<sup>51,52</sup> and quantum scattering<sup>53</sup> calculations on the model Cl + HCl potential energy surface in Ref. 46 predict that rotational excitation of HCl( $v=0$ ) dramatically increases its reactivity. Our results are consistent with this type of effect occurring in I + HI.

In summary, the threshold photodetachment spectra of the  $v_3' = 2$  and 4 peaks observed earlier in the IHI<sup>-</sup> photoelectron spectrum show underlying structure which provides definitive experimental evidence for relatively long-lived metastable states of the [IHI] complex. The spectrum of the  $v_3' = 0$  feature also reveals additional structure which may relate to the reactivity of HI rotational states. This interpretation of our results, if correct, means that even though a linear negative ion is photodetached, we can learn about the non-collinear dynamics of a chemical reaction. The comparison of the new higher resolution results with simulations of the photoelectron spectra is enlightening. On one hand, there are enough areas of agreement to be able to use the simulations in interpreting our data. On the other hand, the discrepancies should aid in constructing a more realistic potential energy surface for the I + HI reaction.

We plan to obtain threshold photoelectron spectra of  $\text{IDI}^-$  in the near future which should provide further insight into the interpretation of our results. In particular, we might expect that the peak spacing of progressions in the symmetric stretch of the [IDI] complex should be similar to the spacing seen in [IHI], whereas structure due to asymptotic I + DI rotational levels should be very sensitive to isotopic substitution.

c)  $\text{IDI}^-(\text{N}_2\text{O})$  Photoelectron Spectrum

An important direction for our photodetachment-based studies of the transition state is the investigation of cluster ions in which a bihalide anion is surrounded by a known number of solvating species, i.e.  $\text{IHI}^-(\text{S}_n)$ . There is no ambiguity concerning the number of solvating species since the ions are mass-selected prior to photodetachment. Photodetachment of the cluster ion generates a neutral collision complex surrounded by the solvating species; such an experiment may serve as a probe of condensed phase reaction dynamics. As a first step to studying larger clusters, we have obtained the photoelectron spectrum of  $\text{IDI}^-(\text{N}_2\text{O})$ , shown in Figure 6. The spectrum was taken at 266 nm.

A comparison of the cluster ion spectrum with the  $\text{IDI}^-$  spectrum in Figure 2 indicates that the addition of an  $\text{N}_2\text{O}$  molecule has perturbed but not destroyed the structure seen in the spectrum of the bare ion. Both spectra show three peaks

assigned to even members of the  $v_3$  progression in the neutral complex. The  $0 \rightarrow 0$  transition is shifted toward lower electron energy by 0.100 eV in the cluster ion spectrum. Assuming that  $N_2O$  interacts much more strongly with  $IDI^-$  than with the  $[IDI]$  complex, then this shift yields the binding energy of  $N_2O$  with  $IDI^-$ . Another difference between the bare and clustered  $IDI^-$  spectra is that the spacing between the three peaks is slightly different. The  $v_3' = 0$  and  $v_3' = 2$  peaks are more widely spaced by 0.013 eV in the  $IDI^-(N_2O)$  spectrum, and the  $v_3' = 2$  and  $v_3' = 4$  spacing is 0.007 eV less than in the bare ion spectrum.

The significance of these results may be best appreciated by considering the previous photoelectron spectroscopy work by Bowen and co-workers<sup>54</sup> on the series  $NO^-$ ,  $NO^-(N_2O)$ , and  $NO^-(N_2O)_2$ . The structure of the  $NO^-$  photoelectron spectrum remains intact in the two cluster ion spectra but shifts towards lower electron kinetic energy by 0.22 eV in the  $NO^-(N_2O)$  spectrum and by 0.48 eV in the  $NO^-(N_2O)_2$  spectrum. These shifts were taken to be the binding energies of one and two  $N_2O$  molecules to  $NO^-$  and are of the same order as the shift seen in the  $IDI^-(N_2O)$  spectrum. However, the small but significant changes in the peak spacing between  $IDI^-$  and  $IDI^-(N_2O)$  were not observed in Bowen's results on the  $NO^-$  series. We believe this variation in the peak spacing results because, in contrast to the stable  $NO$  entity produced in Bowen's experiment, we form an unstable  $[IDI]$  complex which does not have a well-defined equilibrium geometry.

This leads to the following explanation for the different

peak spacings in the  $\text{IDI}^-(\text{N}_2\text{O})$  spectrum. In the cluster ion  $\text{[IDI]}^-(\text{N}_2\text{O})$ , some charge transfer is expected from the  $\text{IDI}^-$  ion to the  $\text{N}_2\text{O}$  molecule. This can distort the  $\text{IDI}^-$  geometry, most likely by lengthening the interiodine distance since the extra electron is what holds the ion together in the first place. On the other hand, subsequent to photodetachment, it is a reasonable approximation to ignore the interaction between the  $\text{[IDI]}$  complex and neighboring  $\text{N}_2\text{O}$  molecule. Thus, the cluster ion photoelectron spectrum is, to first order, equivalent to the photoelectron spectrum of slightly distorted  $\text{IDI}^-$ .

Figure 7 shows a model collinear potential energy surface<sup>42</sup> for the  $\text{I} + \text{DI}$  reaction. The horizontal and vertical axes are proportional to the symmetric and antisymmetric stretch normal coordinates, respectively. The estimated equilibrium interiodine distance in  $\text{IDI}^-$  of  $R_e = 3.88 \text{ \AA}$ <sup>23</sup> corresponds to the solid vertical line drawn through the surface in Figure 7. A cut through the surface at this interiodine distance yields a double minimum potential which is, to a good approximation, the antisymmetric stretch potential for the  $\text{[IDI]}$  complex with an interiodine distance of  $3.88 \text{ \AA}$ . This potential is shown in Figure 8 (solid line), along with the eigenvalues for the first few even  $v_3'$  levels. Suppose that the interiodine distance in  $\text{IDI}^-(\text{N}_2\text{O})$  is  $0.05 \text{ \AA}$  greater than in the bare ion. The antisymmetric stretch potential for the  $\text{[IDI]}$  complex for this geometry is obtained by taking the cut through the surface

indicated by the dashed line in Figure 7. This potential and its first few even eigenvalues are shown in Figure 8 (dashed lines). The major difference between the two potentials is that the barrier between the two minima is higher at larger interiodine distance. While this pushes up all the eigenvalues, the  $v_3' = 2$  level is the most strongly affected since it lies very close to the barrier. The result is that in the antisymmetric stretch potential associated with the cluster ion, the  $v_3' = 0$  and  $v_3' = 2$  levels are further apart, and the  $v_3' = 2$  and  $v_3' = 4$  levels are closer together. This is consistent with the experimentally observed peak spacings.

Thus, our simple picture qualitatively explains the experimental results. The photoelectron of a cluster ion such as  $\text{IDI}^-(\text{N}_2\text{O})$  allows one to probe different regions of the  $\text{I} + \text{DI}$  potential energy surface and also gives an indication of the nature of the interaction in the cluster ion. We plan to study the photoelectron spectra of similar cluster ions in the near future as a function of the type and number of solvating species.

#### SUMMARY

Negative ion photodetachment can provide a detailed probe of the transition state region of a chemical reaction. Examples are presented describing how one can study the  $\text{I} + \text{HI}$  potential energy surface by photodetaching the stable anion  $\text{IHI}^-$ . Results from two types of photodetachment experiments are presented:

photoelectron spectroscopy and threshold photodetachment spectroscopy. The latter, higher resolution technique shows considerably more structure and indicates the presence of relatively long-lived metastable states of the [IHI] complex. Results are also presented for the photoelectron spectrum of the cluster anion  $\text{IDI}^-(\text{N}_2\text{O})$  which probes a different part of the  $\text{I} + \text{DI}$  potential energy surface than the bare ion photoelectron spectrum.

#### ACKNOWLEDGMENTS

The photoelectron spectroscopy work is supported by the Air Force Office of Scientific Research under Grant No. AFOSR-87-0341. The threshold photodetachment studies are supported by the Office of Naval Research Young Investigator Program under Grant No. N0014-87-K-0495.

The results shown here were obtained with the aid of my postdoctoral fellow, Dr. Irene Waller, and my graduate students Don Arnold, Steven Bradforth, Caroline Chick, Doug Cyr, Theo Kitsopoulos, Ricardo Metz, and Alexandra Weaver.

## REFERENCES

1. Okabe, H., *Photochemistry of Small Molecules*, Wiley: New York, 1978.
2. Berkowitz, J., *Photoabsorption, Photoionization, and Photoelectron Spectroscopy*, Academic: New York, 1979.
3. Lykke, K. R., Murray, K. K., Neumark, D. M., Lineberger, W. C., *Phil. Trans. R. Soc. Lond. A*, 324(1988), 179.
4. Arrowsmith, P., Bartoszek, F. E., Bly, S. E., Carrington, T., Charters, P. E., Polanyi, J. C., *J. Chem. Phys.*, 73(1980), 5895.
5. Hering, P., Brooks, P. R., Curl, R. F., Judson, R. S., Lowe, R. S., *Phys. Rev. Lett.*, 44(1980), 687.
6. Maguire, T. C., Brooks, P. R., Curl, R. F., *Phys. Rev. Lett.*, 50(1983), 1918; Maguire, T. C., Brooks, P. R., Curl, R. F., Spence, J. H., Ulvick, S. J., *J. Chem. Phys.*, 85(1986), 844.
7. Grieneisen, H. P., Xue-Jing, H., Kompa, K. L., *Chem. Phys. Lett.*, 82(1981), 421.
8. Wilcomb, B. E., Burnham, R., *J. Chem. Phys.* 74(1981), 6784.
9. Kleiber, P. D., Lyrra, A. M., Sando, K. M., Zafiroopoulos, Z., Stwalley, W. C., *J. Chem. Phys.*, 85(1986), 5493.
10. Benz, A., Morgner, H., *Molec. Phys.*, 57(1986), 319.
11. Nieh, J.-C., Valentini, J. J., *Phys. Rev. Lett.*, 60(1988), 519; *J. Chem. Phys.*, 92(1990), 1083.
12. Buelow, S., Radhakrishnan, G., Catanzarite, J., Wittig, C., *J. Chem. Phys.*, 83(1985), 444; Buelow, S., Noble, M., Radhakrishnan, G., Reisler, H., Wittig, C., Hancock, G., *J. Phys. Chem.* 90(1986), 1015.
13. Breckenridge, W. H., Jouvét, C., Soep, B., *J. Chem. Phys.*, 84(1986), 1443.
14. Imre, D. G., Kinsey, J. L., Field, R. W., Katayama, D. H., *J. Phys. Chem.*, 86(1982), 2564; Imre, D. G., Kinsey, J. L., Sinha, A. Krenos, J., *J. Phys. Chem.*, 88(1984), 3956.
15. Kleinermanns, K., Linnebach, E., Suntz, R., *J. Phys. Chem.*, 91(1987), 5543.
16. Person, M. D., Lao, K. Q., Eckholm, B. J., Butler, L. J., *J. Chem. Phys.*, 91(1989), 812; Lao, K. Q., Person, M. D., Xayaribon, P., Butler, L. J., *J. Chem. Phys.*, 92(1990), 823.

17. Scherer, N. F., Khundkar, L. R., Bernstein, R. B., Zewail, A. H., *J. Chem. Phys.*, 87(1987), 1451; Scherer, N. F., Sipes, C., Bernstein, R. B., Zewail, A. H., *J. Chem. Phys.*, 92(1990), 5239.
18. Dantus, M.; Rosker, M. J., Zewail, A. H., *J. Chem. Phys.*, 87(1987), 2395; Bowman, R. M., Dantus, M., Zewail, A. H., *Chem. Phys. Lett.*, 156(1989), 131; Dantus, M., Bowman, R. M., Gruebele, M., Zewail, A. H., *J. Chem. Phys.*, 91(1989), 7437.
19. Burnett, S. M., Stevens, A. E., Feigerle, C. S., Lineberger, W. C., *Chem. Phys. Lett.*, 100(1982), 124; Ervin, K. M., Ho, J., Lineberger, W. C., *J. Chem. Phys.*, 91(1989), 5974.
20. Moylan, C. R., Dodd, J. A., Han, C., Brauman, J. C., *J. Chem. Phys.* 86(1987), 5350.
21. Ault, B. S., *Acc. Chem. Res.*, 15(1982), 103.
22. Metz, R. B., Kitsopoulos, T., Weaver, A., Neumark, D. M., *J. Chem. Phys.*, 88(1988), 1463.
23. Weaver, A., Metz, R. B., Bradforth, S. E., Neumark, D. M., *J. Phys. Chem.*, 92(1988), 5558.
24. Metz, R. B., Weaver, A. Bradforth, S. E., Kitsopoulos, T. N., Neumark, D. M., *J. Phys. Chem.*, 94(1990), 1377.
25. Schatz, G. C., *J. Chem. Phys.*, 90(1989), 3582; 90(1989), 4847.
26. Bowman, J. M., Gazdy, B. *J. Phys. Chem.* 93(1989), 5129.
27. Gazdy, B., Bowman, J. M., *J. Chem. Phys.*, 92(1989), 4615.
28. Bradforth, S. E., Weaver, A., Arnold, D. W., Metz, R. B., Neumark, D. M., *J. Chem. Phys.*, 92(1990), 7205.
29. Neumark, D. M., in *Electronic and Atomic Collisions- Invited Papers of the XVI ICPEAC* (AIP Conference Proceeding No. 205), edited by A. Dalgarno, R. S. Freund, P. Koch, M. S. Lubell, and T. B. Lucatorto (American Institute of Physics, New York: 1990), pp. 33-48.
30. Bradforth, S. E., Weaver, A., Metz, R. B., Neumark, D. M., in *Advances in Laser Science IV- Proceedings of the 1988 International Laser Science Conference* (AIP Conference Proceedings 191), Gole, J. L., Heller, D. F., Lapp, M., Stwalley, W. C., Eds., American Institute of Physics: New York, 1989, pp. 657-663.
31. Kitsopoulos, T. N., Waller, I. M., Loeser, J. G., Neumark, D. M., *Chem. Phys. Lett.*, 159(1989), 300.

32. Waller, I. M., Kitsopoulos, T. N., Neumark, D. M., *J. Phys. Chem.*, 94(1990), 2240.
33. Leopold, D. G., Murray, K. K., Lineberger, W. C., *J. Chem. Phys.*, 81(1984), 1048, and references therein.
34. Posey, L. A., DeLuca, M. J., Johnson, M. A., *Chem. Phys. Lett.*, 131(1986), 170.
35. Alexander, M. L., Levinger, M. L., Johnson, M. A., Lineberger, W. C., *J. Chem. Phys.*, 88(1988), 6200.
36. Wiley, W. C., McLaren, I. H., *Rev. Sci. Instrum.*, 26(1955), 1150
37. Bakker, J. M. B., *J. Phys E*, 6(1973), 785; 7(1974), 364.
38. Müller-Dethlefs, K., Sander, M., Schlag, E. W., *Z. Naturforsch.*, 39a(1984), 1089; *Chem. Phys. Lett.*, 12(1984), 291.
39. Hotop, H., Lineberger, W. C., *J. Phys. Chem Ref. Data*, 14(1985), 731.
40. Caldwell, G, Kebarle, P., *Can. J. Chem.*, 63(1985), 1399.
41. Huber, K. P., Herzberg, G., *Molecular Spectra and Molecular Structure. IV. Constants of Diatomic Molecules*, Van Nostrand: New York, 1979.
42. Manz, J., Römel, J., *Chem. Phys. Lett.*, 81(1981), 179.
43. Sato, S. *Bull. Chem. Soc. Jpn.*, 28(1955), 450.
44. Based on high resolution gas phase spectra of  $\text{FHF}^-$  (Kawaguchi, K., Hirota, E., *J. Chem. Phys.*, 87(1987), 6838.) and  $\text{ClHCl}$  (Kawaguchi, K., *J. Chem. Phys.*, 88(1988), 4186.)
45. Römel, J., *Chem. Phys.*, 79(1983), 197.
46. Bondi, D. K., Connor, J. N. L., Manz, J., Römel, J., *Molec. Phys.*, 50(1983), 467.
47. Kaye, J. A., Kuppermann, A., *Chem. Phys. Lett.*, 88(1984), 2758.
48. Schatz, G. C., private communication.
49. Gertitschke, P. L., Manz, J., Römel, J., Schor, H. H. R., *J. Chem. Phys.*, 83(1985), 208.
50. Schatz, G. C., *Israel J. Chem.* (in press).

51. Amaee, B., Connor, J. N. L., Whitehead, J. C., Jakubetz, W., Schatz, G. C., *Faraday Discuss. Chem. Soc.*, 84(1987), 387.
52. Kornweitz, H., Broida, M., Persky, A., *J. Phys. Chem.*, 93(1989), 251.
53. Schatz, G. C., *Chem. Phys. Lett.*, 150(1988), 92; 151(1988), 409.
54. Coe, J. V., Snodgrass, J. T., Friedhoff, C. B., McHugh, K. M., Bowen, K. H., *J. Chem. Phys.*, 87(1987), 4302.

## FIGURE CAPTIONS:

**Figure 1.** Photoelectron Spectrum of  $\text{IHI}^-$  at 266 nm. (ref. 32)

**Figure 2.** Photoelectron Spectrum of  $\text{IDI}^-$  at 266 nm. (ref. 29)

**Figure 3.** Threshold photodetachment spectrum of  $v_3 = 2$  peak in  $\text{IHI}^-$  photoelectron spectrum. The points are spaced by 0.1 nm (approximately  $10 \text{ cm}^{-1}$ ). (ref. 32)

**Figure 4.** Threshold photodetachment spectrum of  $v_3 = 4$  peak in  $\text{IHI}^-$  photoelectron spectrum. The points are spaced by 0.1 nm. (ref. 32)

**Figure 5.** Threshold photodetachment spectrum of  $v_3 = 0$  peak in  $\text{IHI}^-$  photoelectron spectrum. The points are spaced by 0.1 nm. The energetic thresholds for the asymptotic levels  $\text{I} + \text{HI}(v=0, j=11-16)$  are indicated, taking the threshold for  $\text{I} + \text{HI}(v=0, j=0)$  to be at 327.14 nm (3.79 eV). (ref. 32)

**Figure 6.** Photoelectron spectrum of  $\text{IDI}^-(\text{N}_2\text{O})$  at 266 nm. (ref. 29).

**Figure 7.** Model collinear potential energy surface for  $\text{I} + \text{DI}$  reaction proposed in ref. 42. The solid vertical line corresponds to estimated interiodine distance  $R_e = 3.88 \text{ \AA}$  in  $\text{IDI}^-$ . The dashed vertical line corresponds to estimated  $R_e = 3.93 \text{ \AA}$  in  $\text{IDI}^-(\text{N}_2\text{O})$ . The modified hyperspherical coordinates  $\rho$  and  $z$  are (approximately) proportional to the symmetric and antisymmetric normal coordinates of the  $[\text{IDI}]$  complex. (ref. 29)

**Figure 8.** Antisymmetric stretch potentials and  $v_3 = 0, 2,$  and  $4$  energy levels for [IDI] complex obtained by cuts through I + DI potential energy surface in Figure 7 at interiodine distances of  $3.88 \text{ \AA}$  (solid lines) and  $3.93 \text{ \AA}$  (dashed lines). (ref. 29)

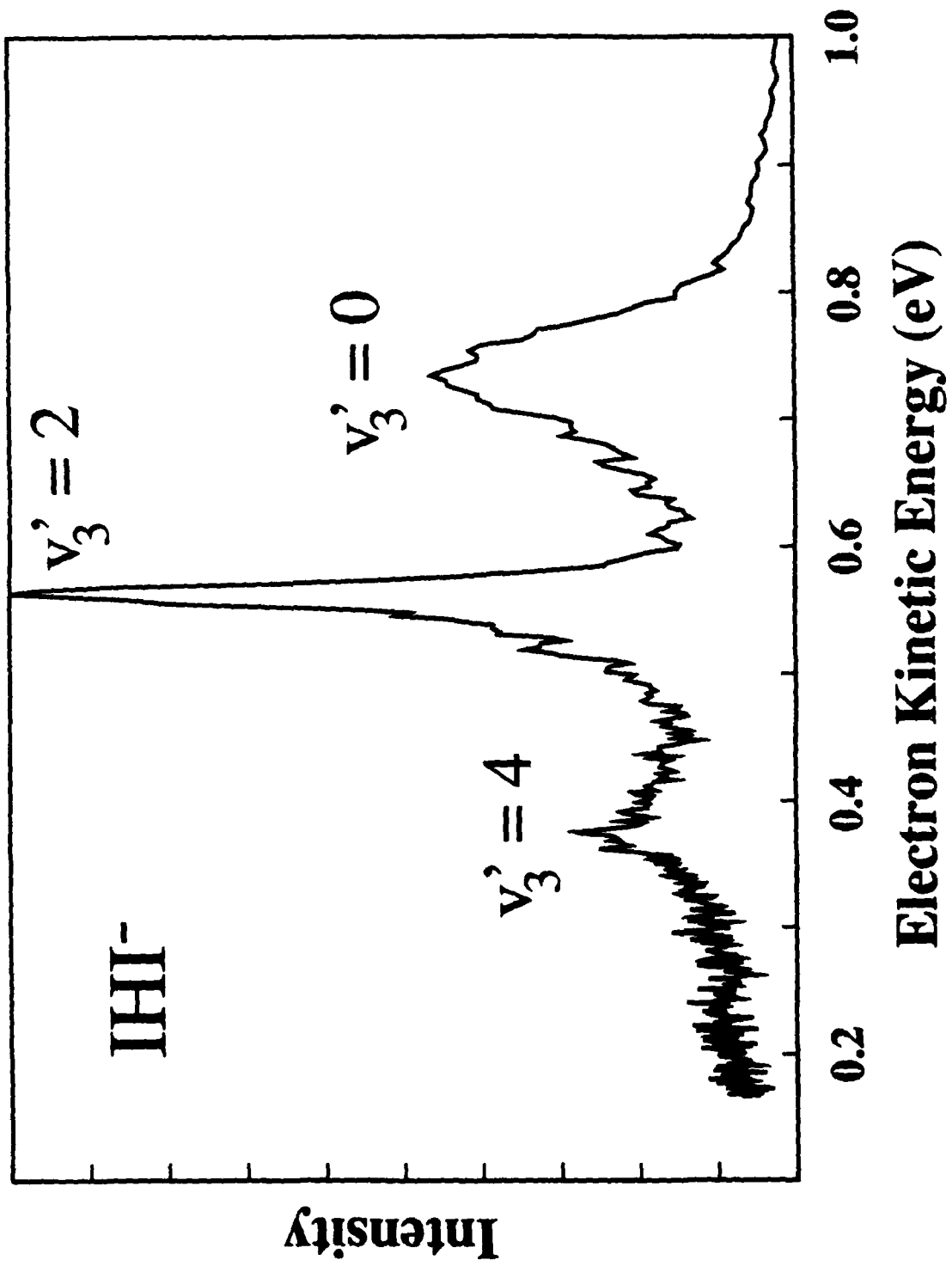


Fig. 1

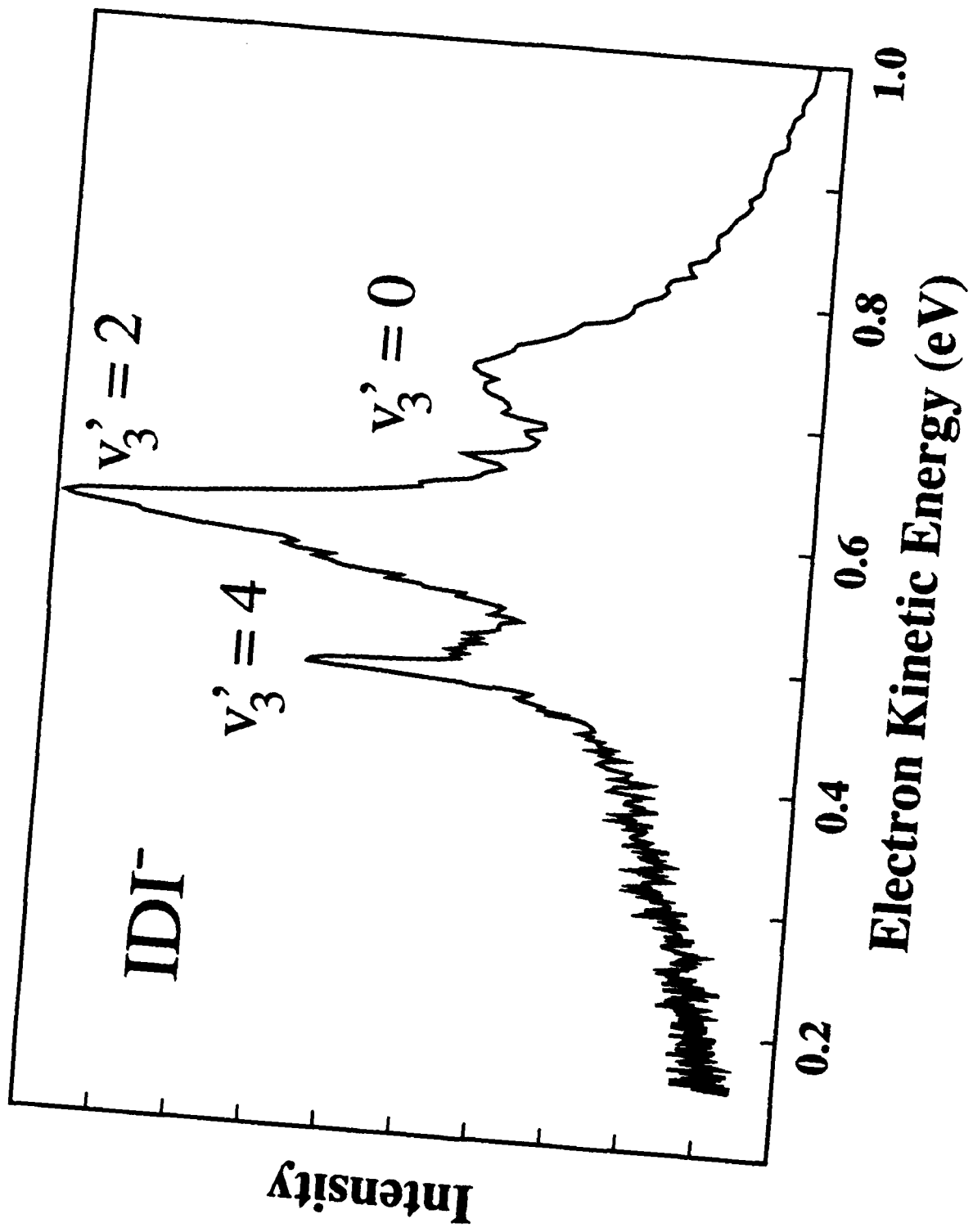


Fig. 2

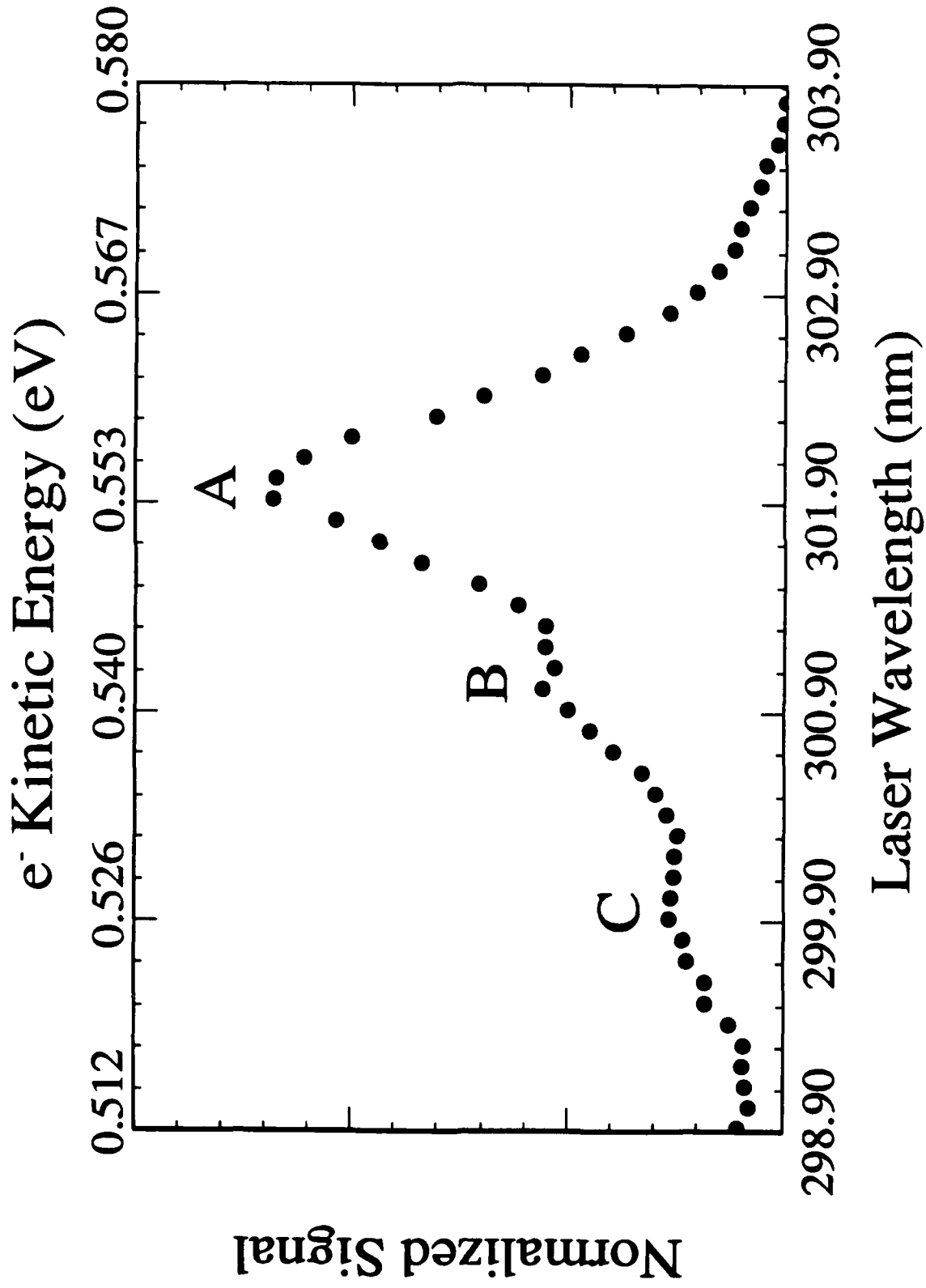


Fig. 3

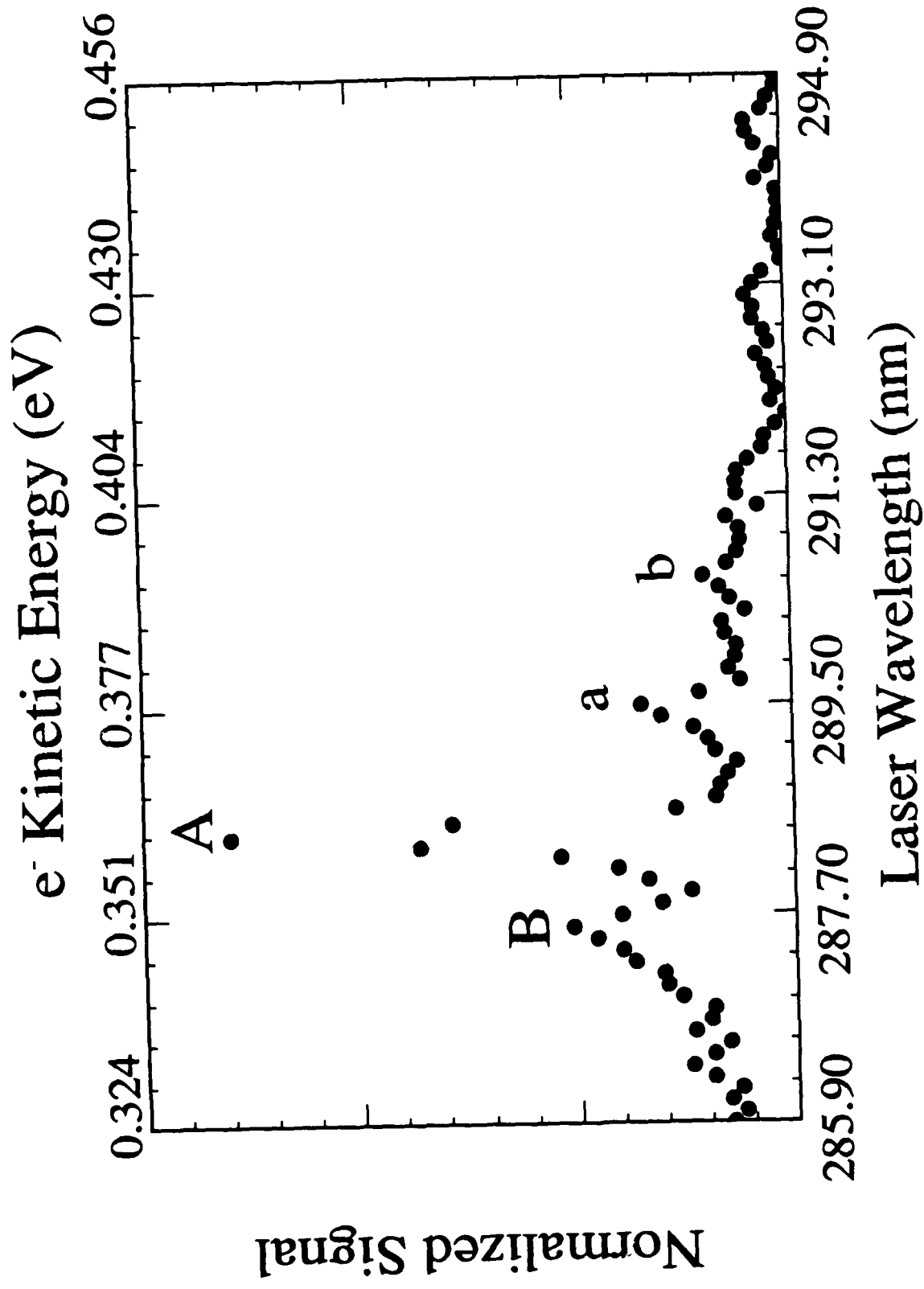


Fig. 4

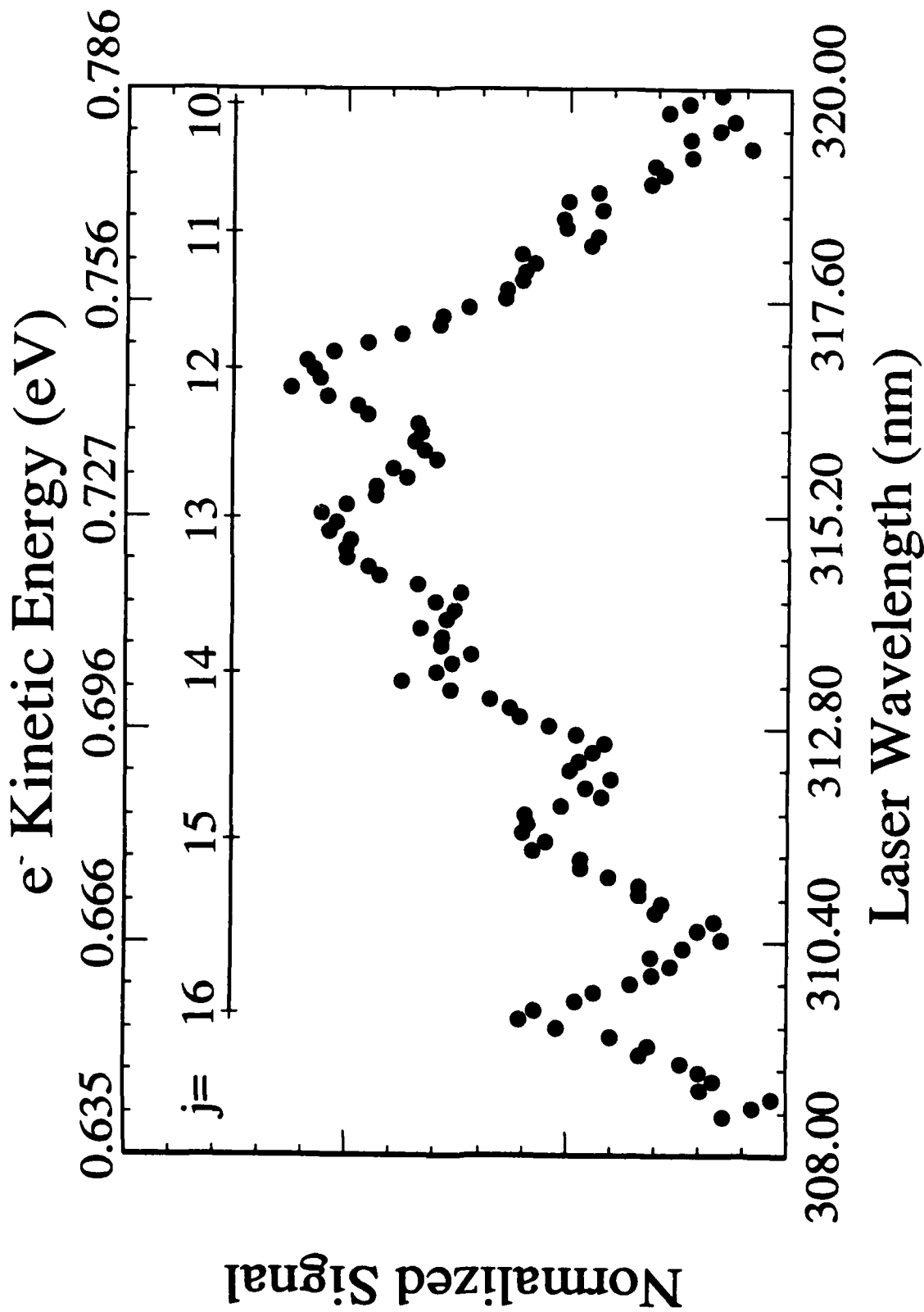


Fig. 5

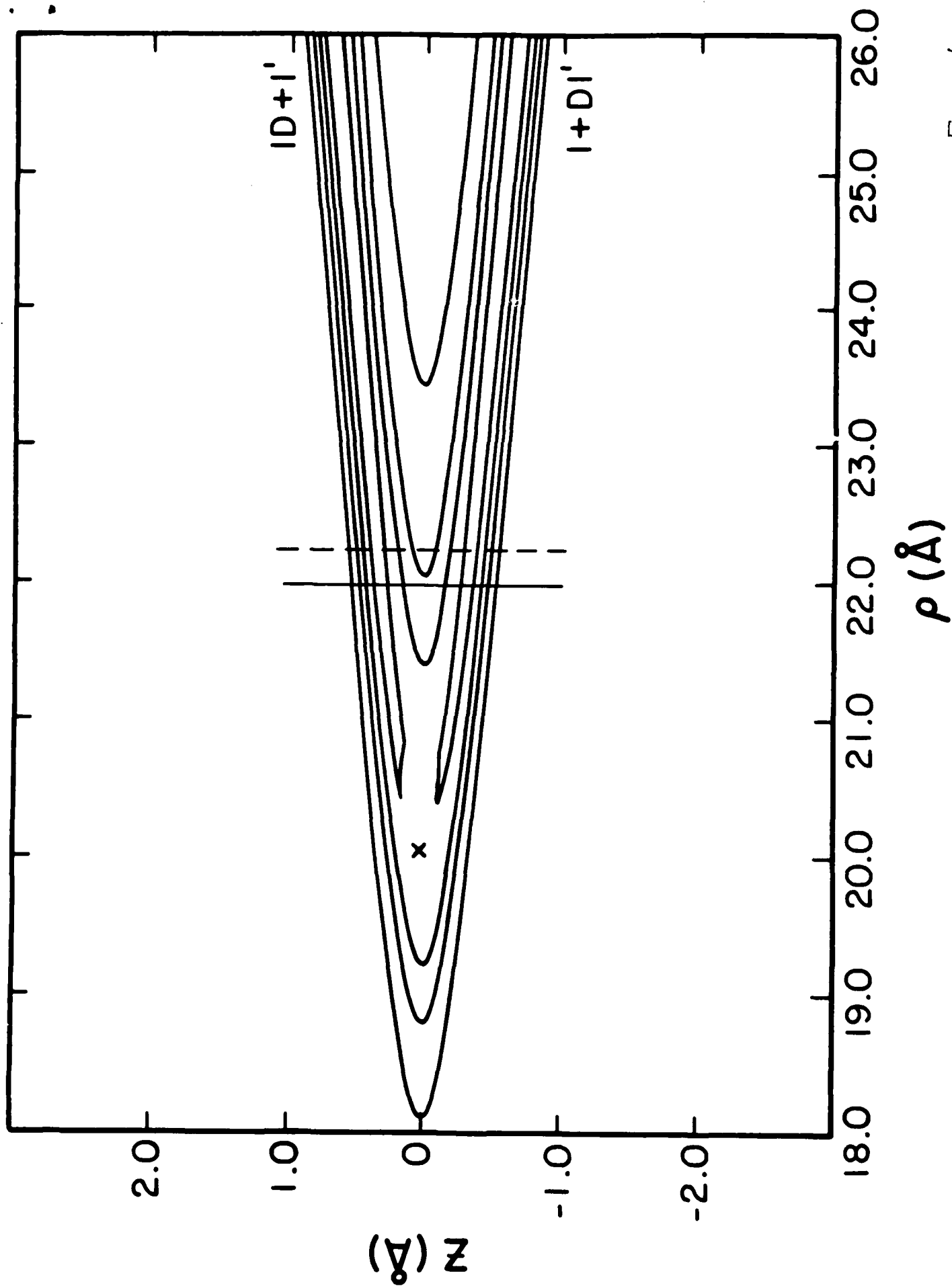
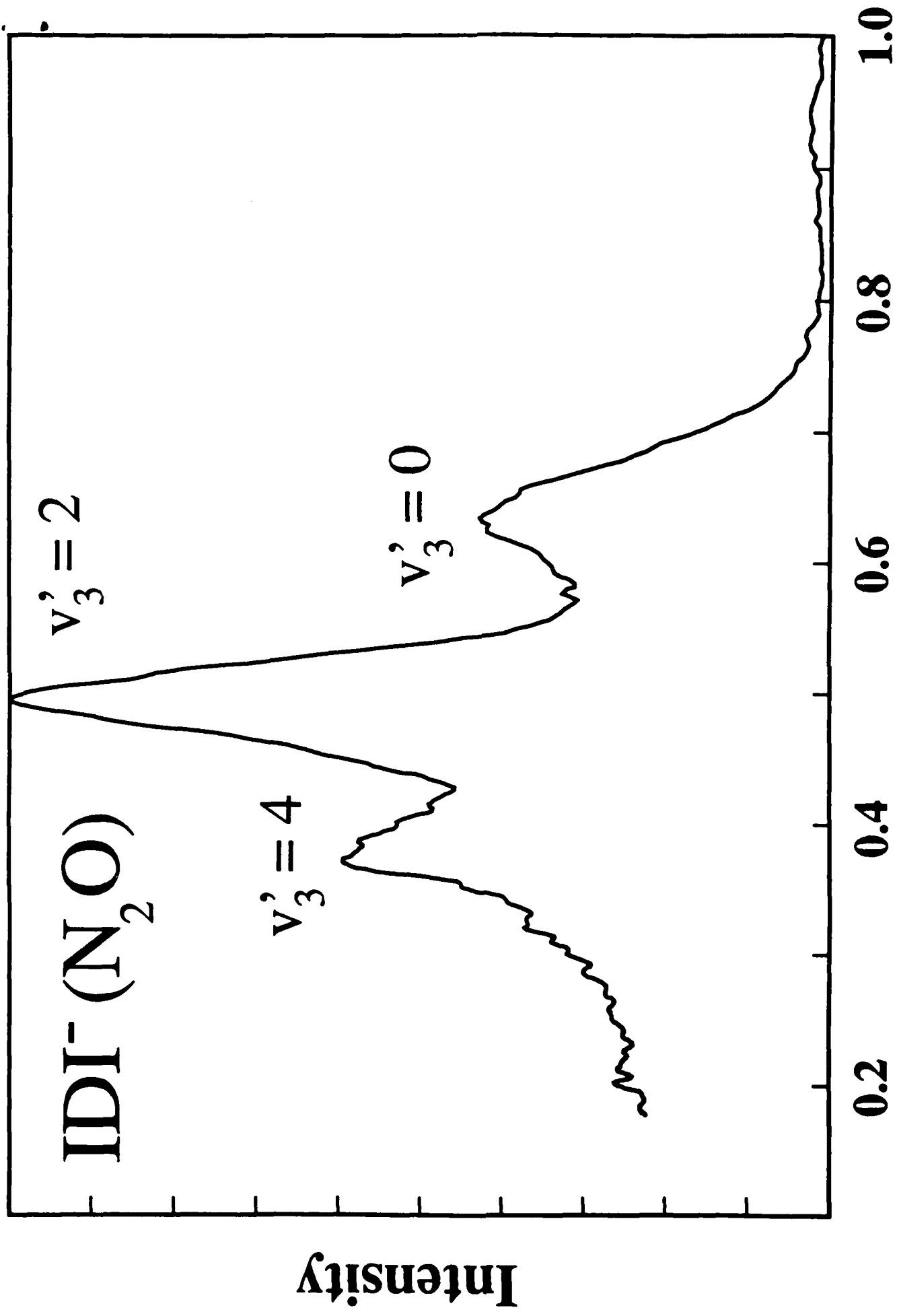


Fig. 6



Electron Kinetic Energy (eV)

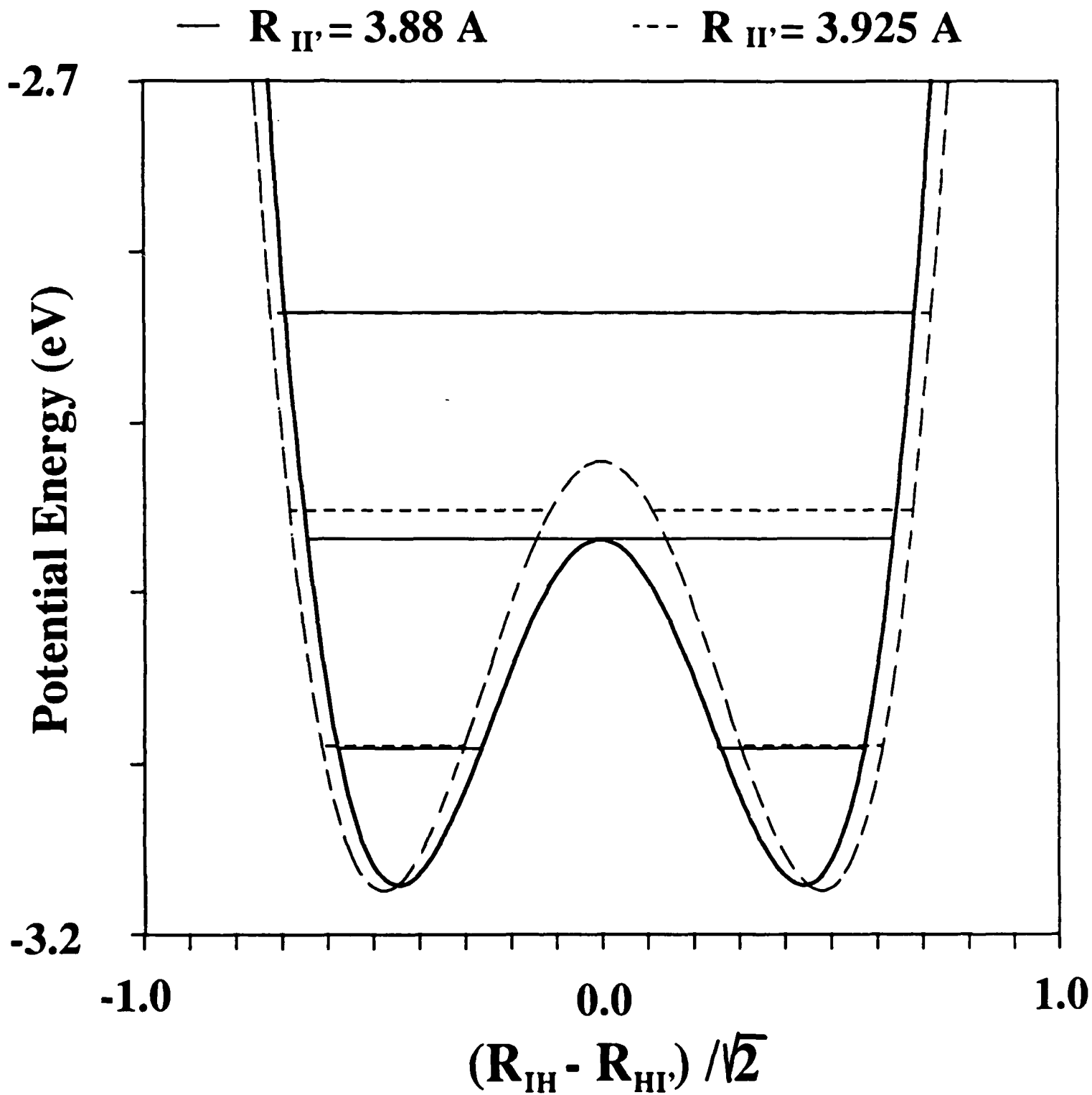


Fig. 8